Gait Phase Subdivision and Leg Stiffness Estimation During Stair Climbing

Teng Ma, *Graduate Student Member, IEEE* , Jiale Zhu, Kuangen Zhang, Wentao Xiao, Haiyuan Liu, Yuquan Leng, Haoyong Yu, *Senior Member, IEEE*, and Chenglong Fu, *Member, IEEE*

***Abstract*—Leg stiffness is considered a prevalent parameter used in data analysis of leg locomotion during different gaits, such as walking, running, and hopping. Quantification of the change in support leg stiffness during stair ascent and descent will enhance our understanding of complex stair climbing gait dynamics. The purpose of this study is to investigate a methodology to estimate leg stiffness during stair climbing and subdivide the stair climbing gait cycle. Leg stiffness was determined as the ratio of changes in ground reaction force in the direction of the support leg F_l (leg force) to the respective changes in length L_l during the entire stance phase. Eight subjects ascended and descended an instrumented staircase at different cadences. In this study, the changes of leg force and length (force–length curve) are described as the leg stiffness curve, the slope of which represents the normalized stiffness during stair climbing. The stair ascent and descent gait cycles were subdivided based on the negative and positive work fluctuations of the center-of-mass (CoM) work rate curve and the characteristics of leg stiffness. We found that the leg stiffness curve consists of several segments in which the force–length relationship was similarly linear and the stiffness value was relatively constant; the phase divided by the leg stiffness curve corresponds to the phase divided by the CoM work rate curve. The results of this study may guide biomimetic control strategies for a wearable lower-extremity robot for the entire stance phase during stair climbing.**

***Index Terms*—Leg stiffness, stair ascent, stair descent, human walking, phase subdivision.**

Manuscript received October 18, 2021; revised January 10, 2022; accepted March 21, 2022. Date of publication March 29, 2022; date of current version April 5, 2022. This work was supported in part by the National Natural Science Foundation of China under Grant U1913205 and Grant 62103180; in part by the National Key Research and Development Program of China under Grant 2018YFC2001601; in part by the Guangdong Basic and Applied Basic Research Foundation under Grant 2020B1515120098; in part by the Guangdong Innovative and Entrepreneurial Research Team Program under Grant 2016ZT06G587; in part by the Science, Technology and Innovation Commission of Shenzhen Municipality under Grant SGLH20180619172011638, Grant ZDSYS20200811143601004, and Grant KQTD20190929172505711; in part by the Stable Support Plan Program of Shenzhen Natural Science Fund under Grant 20200925174640002; in part by the Agency for Science, Technology and Research, Singapore, under the National Robotics Program, with A*star Science and Engineering Research Council (SERC) under Grant 192 25 00045; and in part by the Centers for Mechanical Engineering Research and Education at the Massachusetts Institute of Technology (MIT) and the Southern University of Science and Technology (SUSTECH). *(Corresponding author: Chenglong Fu.)*

This work involved human subjects or animals in its research. Approval of all ethical and experimental procedures and protocols was granted by the Southern University of Science and Technology (SUSTech) Medical Ethics Committee under Approval No. 20210009.

Teng Ma is with the Shenzhen Key Laboratory of Biomimetic Robotics and Intelligent Systems and the Guangdong Provincial Key Laboratory of Human-Augmentation and Rehabilitation Robotics in Universities, Department of Mechanical and Energy Engineering, Southern University of Science and Technology, Shenzhen 518055, China, and also with the Department of Biomedical Engineering, National University of Singapore, Singapore 119077.

Jiale Zhu, Wentao Xiao, Haiyuan Liu, Yuquan Leng, and Chenglong Fu are with the Shenzhen Key Laboratory of Biomimetic Robotics and Intelligent Systems and the Guangdong Provincial Key Laboratory of Human-Augmentation and Rehabilitation Robotics in Universities, Department of Mechanical and Energy Engineering, Southern University of Science and Technology, Shenzhen 518055, China (e-mail: fucl@sustech.edu.cn).

Kuangen Zhang is with the Shenzhen Key Laboratory of Biomimetic Robotics and Intelligent Systems and the Guangdong Provincial Key Laboratory of Human-Augmentation and Rehabilitation Robotics in Universities, Department of Mechanical and Energy Engineering, Southern University of Science and Technology, Shenzhen 518055, China, and also with the Department of Mechanical Engineering, The University of British Columbia, Vancouver, BC V6T1Z4, Canada.

Haoyong Yu is with the Department of Biomedical Engineering, National University of Singapore, Singapore 119077.

Digital Object Identifier 10.1109/TNSRE.2022.3163130

I. Introduction

STAIR climbing is one of the most common activities in daily living. Walking on stairs presents as more demanding than level walking, especially for the elderly [1], [2], subjects suffering from muscle or joint diseases [3], [4], and subjects with amputations [5]–[9]. The studies of biomechanics of stair climbing can enhance our understanding of the complicated processes of human locomotion during stair ascent and descent. Furthermore, the biomechanical analysis of normal stair climbing can support the design and control of rehabilitation devices, such as lower-extremity exoskeletons or prostheses [10]–[15].

Previous studies investigated the biomechanics of normal human ascending and descending stairs [16]–[22]. Biomechanical parameters commonly used in locomotion analysis include joint angles and moments [23], joint power [24], grand plantar pressure characteristics [25], foot clearance [26], whole-body angular momentum [27], and ground reaction forces (GRFs) [28]. Other related works show that dual-tasking affects the kinetics but not the kinematics of stair climbing [29], that stair inclinations significantly influence the joint powers [30], and that different-level steps result in different joint moments in both sagittal and frontal planes [31]. In addition, some researchers have focused on the biomechanical analysis of stair ambulation in the elderly [32], lower-limb amputees [33], and people with joint disease [34], which contributes to the design of low-extremity exoskeletons and prostheses.

Stair climbing presents a greater biomechanical challenge relative to level walking because the body CoM must be raised during ascent and lowered during descent during the single-limb stance phase while maintaining forward progression and proper foot placement. It is reported that the stance phase occupies approximately 60% of the gait cycle in stair ascent or descent, and the performance of the swing phase depends on the stance phase [35]. Therefore, the biomechanical characteristics of the stance phase during stair climbing are essential in studies on stair climbing. Leg stiffness is a key parameter in data analysis of legged locomotion during the stance phase [36], [37], and several studies have investigated leg stiffness during level walking [38], [39], running [40], [41], and hopping [42]. To the best of author's knowledge, few comprehensive analyses have discussed leg stiffness during stair climbing, although leg stiffness while stair climbing is an important characteristic affecting gait kinetics and the kinematics of stair climbing [43]. Furthermore, leg stiffness in previous studies was mostly regarded as a single constant value that could be simulated accurately by vertical directional models. The leg stiffness is calculated as the ratio of maximum value of the ground reaction forces to maximum displacement of COM during body contact with the ground [38]–[42], [44]. However, stair climbing is a relatively complex movement, with several phases alternating and leg stiffness changing during different phases. To investigate leg stiffness during different phases, it is necessary to further define the subphases of stair ascent and descent. The gait cycle during stair climbing was divided into phases according to different objectives for progression [45]. Based on the actions of CoM and GRF, [35] further refine the phases described by [45]. In this study, negative and positive work fluctuations of the CoM work rate curve are used to subdivide phases of stair climbing, which reveals the change of mechanical energy during stair climbing. The changes in mechanical energy and quantification of leg stiffness during different phases may guide biomimetic control strategies for a wearable lower-extremity robot for the entire stance phase during stair climbing.

The purposes of this study are to explore the body CoM work rate and leg stiffness during stair climbing, subdivide stair climbing gait phases, and investigate how stair climbing speed affects leg stiffness variation. The main contributions of this paper are summarized as follows.

(1) This study reveals *variable leg stiffness* of the supporting leg at different phases during the complex process of stair climbing, which changes continuously in different phases and remains relatively constant in each phase.

(2) Stair climbing gait phases are subdivided based on the negative and positive work fluctuations of CoM work rate and the characteristics of leg stiffness. The stance phase of stair ascent includes five subphases: *collision*, *early lifting*, *late lifting*, *strutting*, and *push-off*, and the stance phase of stair descent includes four subphases: *collision*, *rebound*, *early transition*, and *late transition*.

(3) The *variable leg stiffness* of different phases and speeds during stair climbing is estimated based on the profile of the leg force–length curves rather than the peak values of force and length used in previous studies. These results can serve as a reference for the imitation of natural motor control strategies in prostheses or exoskeletons applied to stair climbing.

TABLE I
VECTOR NOTATION

Variable	Notation
Position vector	$\boldsymbol{r}$
Ground reaction force	$\boldsymbol{GRF}(GRF_x, GRF_y, GRF_z)$
Leg force	$\boldsymbol{F_l}$
Leg force (scalar)	$F_l = \lvert\boldsymbol{F_l}\rvert$
Length (scalar)	$L_l = \lvert\boldsymbol{r}\rvert$

II. METHOD

A. Protocols

Eight healthy subjects (23 ± 3 years old) of similar body height (1.72 ± 0.10 m) and weight (72.5 ± 8.5 kg) participated in this study and completed the informed consent approved by the Institutional Review Board of Southern University of Science and Technology. In a questionnaire, subjects reported no history of leg injuries or balance disorders and reported they could execute stair ascent and descent at different cadences.

The subjects walked up and down the instrumented staircase at three cadences (80, 90, and 100 steps/min). For each subject and for each cadence, ascend and descend movements were recorded for three repetitive trials. Stair ascent was initiated in front of the staircase on ground level, whereas stair descent started on a platform. Prior to data acquisition, the subjects ascended and descended the stairs several times until they were accustomed to the motion.

B. Measurement

The instrumented staircase consisted of eight steps with a force plate (FP4060-08, Bertec, Columbus, OH, USA) embedded in each step. The step dimensions were 15 cm (rise) by 30 cm (run), and the steps were wide enough (150 cm) to avoid falling.

For each trial, body kinematics and kinetics were captured by 12 motion-capture cameras (Motion Analysis, Raptor-12HS, Rohnert Park, CA, USA) and the instrumented stairs, with a sampling frequency of 120 Hz for the motion-capture cameras and 1200 Hz for the force plates. The force plates can measure F_l, including the force magnitude, direction, and starting point of the center of pressure (CoP). Fifteen reflective markers were placed on the V-Sacral and lower limbs. Three markers were used (L-ASIS, R-ASIS, and V-Sacral) from the Halen Hayes model to assist in CoM tracking, and hence the CoM was replaced by the center of pelvis calculated by the three markers [46]. Using the Motion Analysis System and force plates, we can obtain the data of human lower-extremity motion and the force F_l synchronously [47], [48]. Motion-capture and force-plate data were filtered by a fifth-order Butterworth lower-pass filter with cutoff frequencies of 10 and 30 Hz, respectively. As shown in Table I, vector $\boldsymbol{r}$ is the

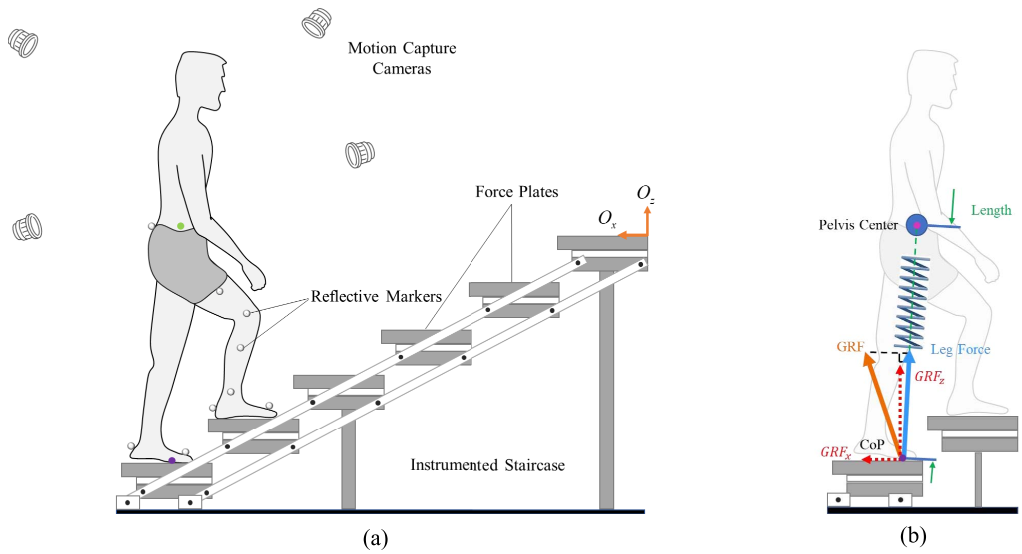

Fig. 1. Testing environment and description of parameters of selected support leg. (a) Testing equipment includes motion-capture cameras, instrumented stairs with force plates, and subjects walking on stairs wearing reflective markers. (b) Virtual limb length is the distance between the pelvis center and center of pressure (CoP), and leg force is the ground reaction force (GRF) component in the direction of CoP to CoM.

position vector from the CoP to the pelvis, the length L_l was defined as the nominal value of $\boldsymbol{r}$. The leg force F_l is the component of the GRF in the direction of the position vector $\boldsymbol{r}$, as shown in Fig. 1(b).

C. Analysis

To cover the individual differences, the leg force and virtual limb length were normalized by follows.

$$F_N = F_l/mg, \tag{1}$$
$$L_N = L_l/L_0, \tag{2}$$

where m is the body mass; L_0 represents the initial leg length, defined as the distance from the CoM to the CoP while standing upright. During stair climbing, CoM velocity was determined by the integration of the leg forces, considering periodic strides and steady state. Furthermore, the support CoM work rate was calculated from the vector dot product of the leg force F_N with the velocity of the CoM [49], [50] as

$$\begin{aligned} P_{\mathrm{CoM}} &= \vec{F}_N \cdot \vec{V}_{\mathrm{CoM}} \\ &= |F_N||V_{\mathrm{CoM}}|\cos\theta \\ &= |F_N||V_{\mathrm{leg}}|, \end{aligned} \tag{3}$$

where P_{CoM} and V_{CoM} are CoM work rate and CoM velocity, respectively. The CoM velocity was decomposed into the direction of the position vector $\boldsymbol{r}$ (V_{leg}) and the direction perpendicular to the vector $\boldsymbol{r}$. As F_N is along the direction of the vector $\boldsymbol{r}$, the CoM work rate is equal to zero when the virtual limb length changing velocity is zero.

Based on the experimental results, the F_N-L_N curve and CoM work rate curve were used to analyze the leg stiffness and CoM work done during stair climbing at different speeds. Furthermore, the gait cycle during stair climbing can be divided into several portions based on the F_N-L_N curve and CoM work rate curve. The leg stiffness of different phases during stair climbing was calculated based on the profile of the F_N-L_N curve. It should be noted that the leg stiffness termed in this study is "*quasi-leg stiffness*" [51], [52] due to the contribution of inertia and damping to the final results.

D. Statistical Analysis

All statistical analyses were performed using IBM SPSS Statistics version 20.0. Normal distribution for each variable was assessed using the Shapiro–Wilk test and the Anderson–Darling test. In cases of non-normal distribution, a log transformation was completed, and normal distribution was reevaluated. To statistically confirm differences between different gait speeds in the different gait phases, we applied the Mann-Whitney U test to these variables and two-way ANOVA [5 phase × 3 speed (stair ascent), 4 phase × 3 speed (stair descent)] to find the difference of leg stiffness at different gait speeds in different gait phases. The significance level was set at 0.05.

III. Results

A. Stair Ascent Gait Cycle Subdivision

In this study, the stair climbing stance phase can be first divided into different subphases according to the CoM work rate. The direction of the leg force F_N and CoM velocity V_{CoM} during different subphases of stair ascent are shown in Fig. 2(a). In the CoM work rate curve, the zero points B, C, and D (except the starting point A and ending point E of the stance phase) at which the curves cross over the X axis are the demarcations of the subphases in the stance phase. Based on the gait events and CoM work rate curve, the stance phase can be divided into four subphases, including the collision, lifting, strutting, and push-off, as shown in Fig. 2(b). Similar to the CoM work rate curve, the F_N-L_N curve can also be divided into several parts according to the inflection points B, C, and D of the curve, as shown in Fig. 2(c). The slope of each part

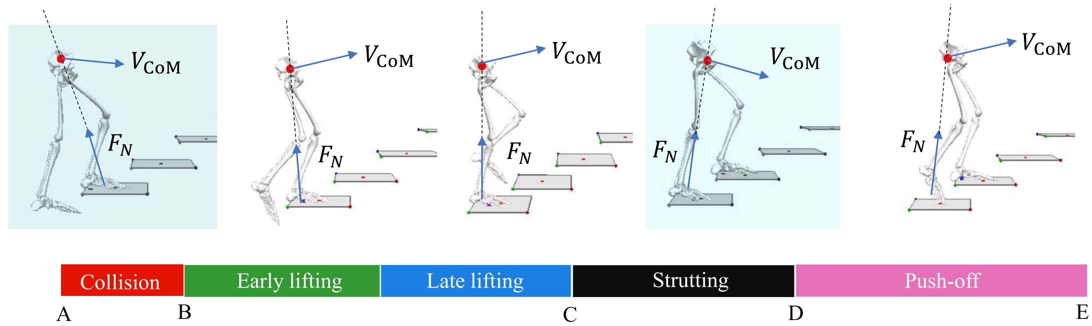

(a) Schematic of F_N and V_{CoM} during stair ascent

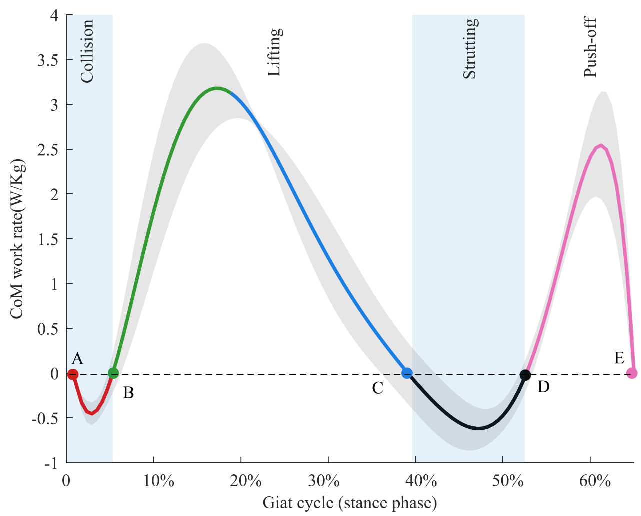

(b) Stair ascent CoM work rate curve

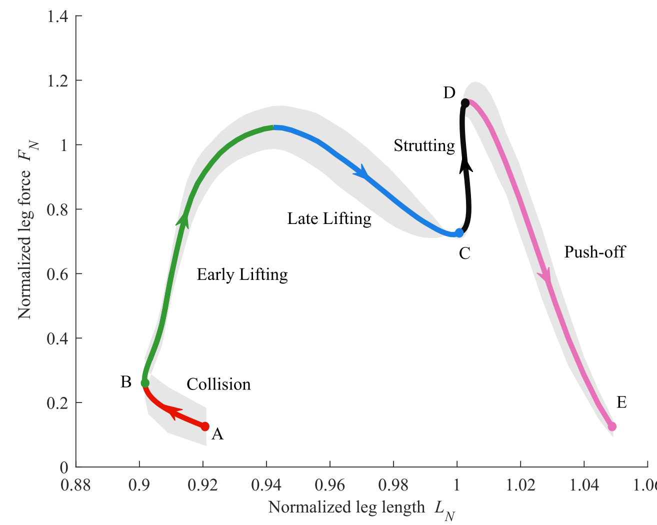

(c) Stair ascent leg stiffness curve

Fig. 2. Stair ascent gait cycle subdivision based on CoM work rate and leg stiffness, averaging all trials across subjects with standard deviations (± 1) indicated by shaded regions. (a) Stair ascent stance phase diagram. (b) CoM work rate curve divided into four subphases by points A, B, C, D, and E. (c) $F_N - L_N$ curve divided into the same four subphases. Different subphases correspond to different slopes and features.

represents the leg stiffness during this subphases. Moreover, the inflection points in the F_N-L_N curve correspond to the zero points in the CoM work rate, because the virtual limb length change velocity at the inflection point is zero. Therefore, during different subphases of stair ascent, the CoM work rate followed a pattern of positive and negative work fluctuations, while the leg stiffness was also constantly changing.

The four subphases including collision, lifting, strutting, and push-off directly reflected the performances of the support leg during stair ascent. The collision phase begins with stair contacting by one foot, as point A shown in the F_N-L_N curve, with the virtual lower limb length decreasing as the foot collides with the step, and ends with the opposite foot leaving the step. At this moment, the length reaches the first minimal value, as shown by point B in Fig. 2(c). During the collision, the energy is partially stored in the leg compression and will release in the lifting phase to lift the body up to enter the single stance phase and climb the step. The lifting phase starts from the first minimal value of the virtual lower limb length, and ends at the first maximal value of the virtual lower limb length, as shown by point C in Fig. 2(c). During the lifting, the body mainly does positive work through the hip-knee joint to overcome gravity to lift the CoM, and therefore the CoM work rate curve displays a region of positive work. The virtual lower limb length increases uniformly, and according to the changing trend of leg force it can be divided into early lifting and late lifting. The strutting phase starts from the first maximal value of the virtual lower limb length (point C) to the second minimal value of the virtual lower limb length (point D). During the strutting, the CoM moves from the back of the CoP to the front, the contra-lateral foot moves from the swing phase to contact the stair, and the F_N performs negative CoM work. The leg is fully extended like a strut and the length of the leg barely changes. Finally, the push-off phase starts from the second minimal value of the virtual lower limb length, until the end point of the stance phase (point E), that is, the toe off of the support leg. During this phase, the subject lifts the body by flexing the ankle plantar; the foot leaves the steps and enters the swing phase, with the opposite leg in the early lifting phase.

B. Stair Descent Gait Cycle Subdivision

Similar to the study of stair ascent, the change in CoM work rate and leg stiffness were also investigated during different subphases of stair descent, as shown in Fig. 3. According to

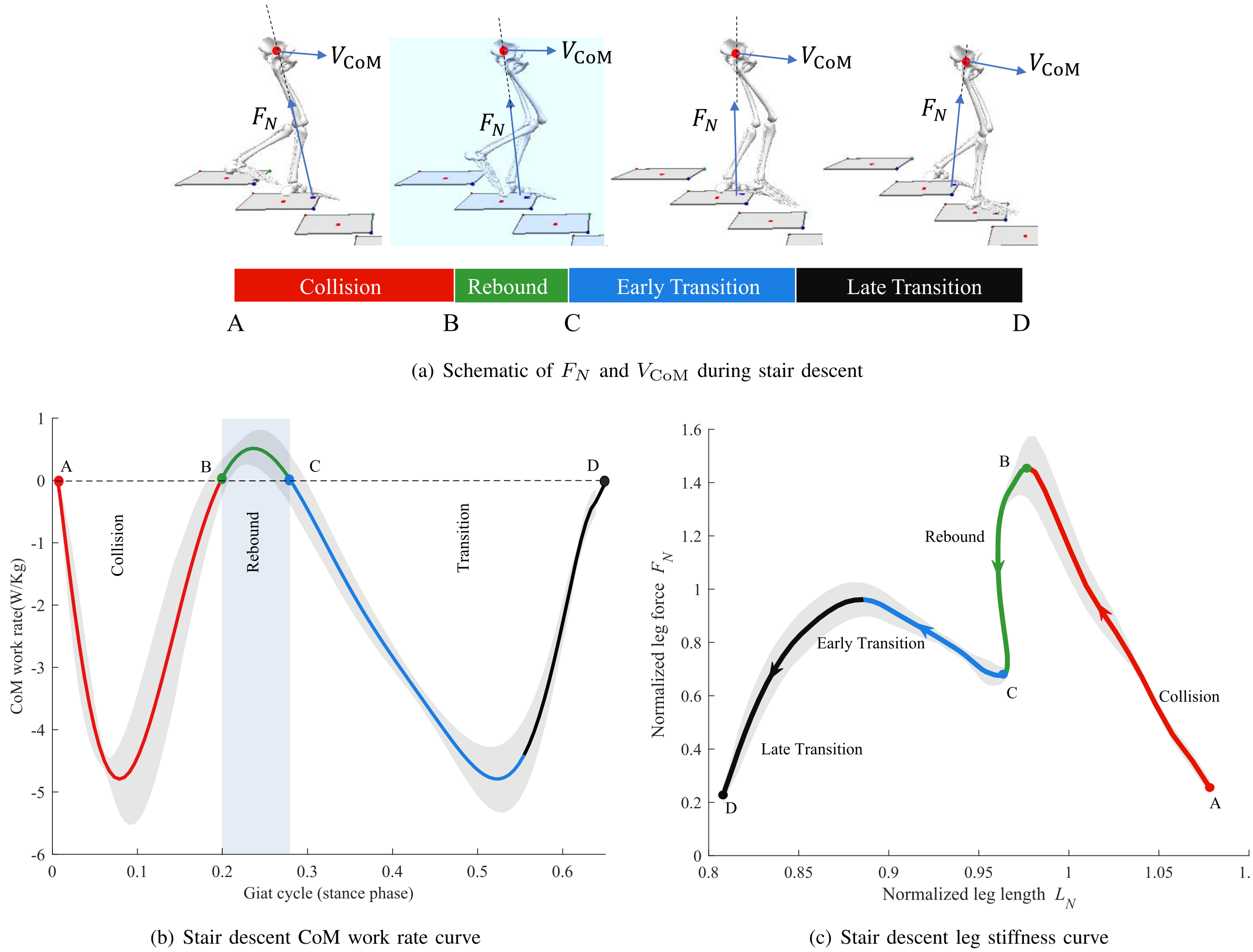

Fig. 3. Stair descent gait cycle subdivision based on CoM work rate and leg stiffness, averaging all trials across subjects with standard deviations (± 1) indicated by shaded regions. (a) Stair descent stance phase diagram. (b) CoM work rate curve divided into three subphases by points A, B, C, and D. (c) $F_N - L_N$ curve divided into the same three subphases. Different subphases have different slopes and features.

the stair descent CoM work rate curve [Fig. 3(b)] and the $F_N - L_N$ curve [Fig. 3(c)], the stair descent stance phase was divided into three subphases, including collision, rebound, and transition. Similar to stair ascent, the collision phase of stair descent starts with one foot contacting the stair [point A in Fig. 3(c)], with the length decreasing as the foot collides with the step, and ending when the opposite foot begins to leave the stair [collision phase in Fig. 3(b) and point B in Fig. 3(c)]. During the collision, the subject starts to contact the stair with the frontal foot, relying on the elasticity of the joint to absorb the energy of impact and play the role of a buffer, and performs negative CoM work [Fig. 3(b)]. Unlike stair ascent, the collision phase comprises a large proportion of the total gait cycle of stair descent (stair ascent 5% and stair descent 20%), which also requires more energy to dissipate. For the rebound phase, the energy stored during the collision phase will release and lead to a small positive CoM work. Since the virtual limb length changes little over this phase, the supporting leg bears the majority of the body's weight, the GRF increases quickly, and the leg is also rigid like a strut. Finally, in the transition phase, the CoM falls and moves forward while preparing for the landing of the contra-lateral foot. The bend of the knee joint and dorsiflexion of the ankle joint lead to the decrease of the virtual limb length. The CoM moves along the direction of leg contraction, which shows a negative work rate. According to the changing trend of leg force, this phase can be divided into early transition and late transition.

C. Leg Stiffness During Different Phases of Stair Climbing

Compared with the previous studies on leg stiffness, the change of leg force and length are described as the $F_N - L_N$ curve in this study, the slope of which represents the normalized stiffness during stair climbing. As shown in Fig 2(c), the collision phase curve AB rises slowly, and its slope illustrates that the leg stiffness increases gradually over this phase. The lifting phase is divided into early lifting and late lifting based on the change of slope. The early lifting phase curve is gradually flattened, which shows that the leg stiffness decreases gradually. The slope of the late lifting curve nearly remains constant, and therefore the leg stiffness is almost unchanged during this phase. Regarding the strutting phase, the curve CD is nearly vertical upward, which means that the

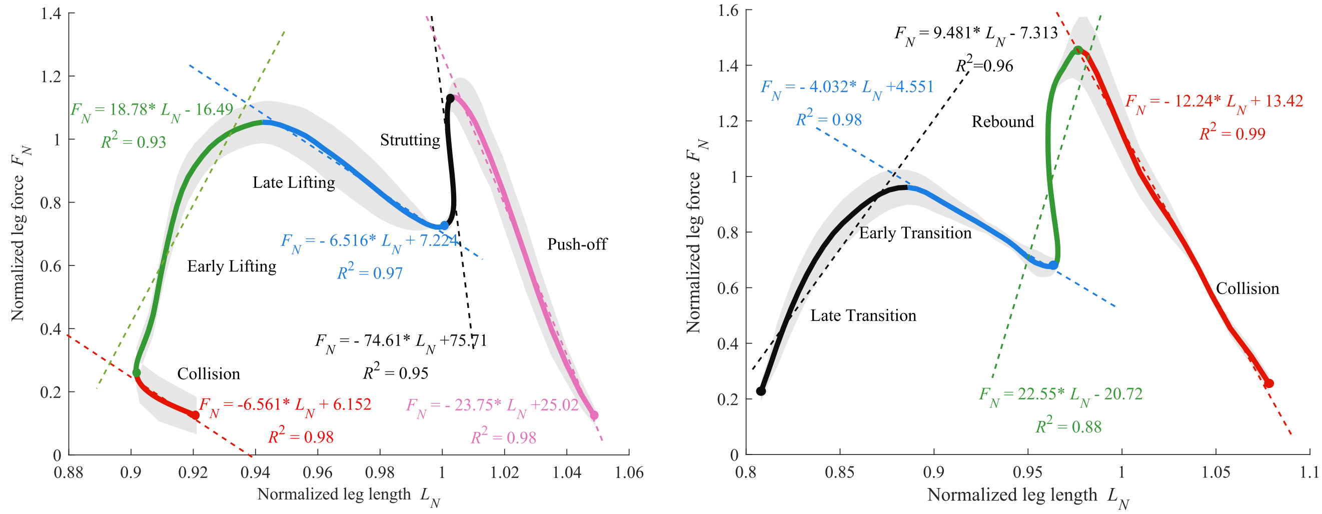

(a) Stair ascent leg stiffness estimation

(b) Stair descent leg stiffness estimation

Fig. 4. Estimation of leg stiffness at different phases during stair ascent and descent. (a) Stair ascent leg stiffness estimation based on the profile of the $F_N - L_N$ curve. (b) Stair descent leg stiffness estimation based on the profile of the $F_N - L_N$.

leg stiffness is extremely large and the leg performs like a strut. Finally, the push-off phase is a nearly linear oblique line, which represents the continuous and steady process of pushing the toe off the ground and pushing the body upward and forward, while the leg stiffness remains almost constant.

During stair descent [Fig. 3(c)], the F_N-L_N curve is almost linear over the collision phase, which indicates that the values of leg stiffness are relatively constant. Similar to strutting phase during ascent, the leg performs like a strut and the leg stiffness is extremely large. The transition phase is also divided into early transition and late transition based on the leg stiffness characteristics, and the leg stiffnesses of the two phases are also relatively constant.

Although the leg stiffness changes during each subphases, it can be observed that the relationship of $F_N - L_N$ is similarly linear and the stiffness value is relatively constant. Therefore, in this study the leg stiffness of different phases is estimated based on the profile of the $F_N - L_N$ curves. As shown in Fig. 4, the dotted lines along each part of the curve are a linear fitting of the corresponding part, the slopes of which are the estimations of normalized leg stiffness of each phase. The values of determination coefficient R^2 that represent the quality of model match. The absolute leg stiffness can be calculated as

$$K = K_{\text{nom}} \cdot mg/L_0, \quad (4)$$

where K_{nom} denotes the normalized leg stiffness and K the absolute leg stiffness. Tables II and III show normalized leg stiffness and absolute leg stiffness at different phases of stair ascent and descent, respectively. The force-length curves reveal the variable leg stiffness during stair climbing, as opposed to the single constant value used in previous studies to describe the leg stiffness during different locomotion.

TABLE II
STAIR ASCENT LEG STIFFNESS OF DIFFERENT PHASES

	Collision	Early lifting	Late lifting	Strutting	Push-off
K_{nom}	6.56	18.78	6.52	74.61	23.75
K (KN/m)	5.07	14.50	5.04	57.62	18.34

TABLE III
STAIR DESCENT LEG STIFFNESS OF DIFFERENT PHASES

	Collision	Rebound	Early transition	Late transition
K_{nom}	12.24	22.55	9.48	4.03
K (KN/m)	9.45	17.41	7.32	3.11

D. Stair Ascent and Descent at Different Speeds

It has been presented in another study that leg stiffness can be influenced by locomotion speed [53]. Stair climbing at different cadences were performed to investigate the effect of speed on the work performed and leg stiffness over each gait cycle. During stair ascent and descent, the leg stiffness and CoM work generally increased with speed. It was obvious that the CoM work increased with speed during different subphases of stair ascent and descent ($p < 0.05$), as shown in Fig. 5(a) and (b). The profile of the $F_N - L_N$ curve at different stair climbing speeds is very similar [Fig. 5(c) and (d)]. A quantitative comparison of the leg stiffness during different subphases of stair ascent and descent revealed notable trends with different stair climbing speeds, as shown in Fig. 5(e) and (f). As shown in Fig. 5(e), because the leg performs like a strut, the magnitudes of leg stiffness during the strutting phase are significantly larger than in the other phases. Statistical analysis revealed that the leg stiffness during different phases is significantly different ($p < 0.05$), which again indicates that the stiffness of each phase during stair climbing is different and cannot be described by a single constant value. Overall, the leg stiffness increases with speed ($p < 0.05$) during stair ascent except for strutting phase. Similarly, the leg stiffness during the rebound phase is significantly larger than in the other phases during stair descent (Fig. 5(f)). Statistical analysis reported that no significant difference in leg stiffness between speeds during rebound phase, and leg stiffness increases with speed during other phases of stair descent ($p < 0.05$).

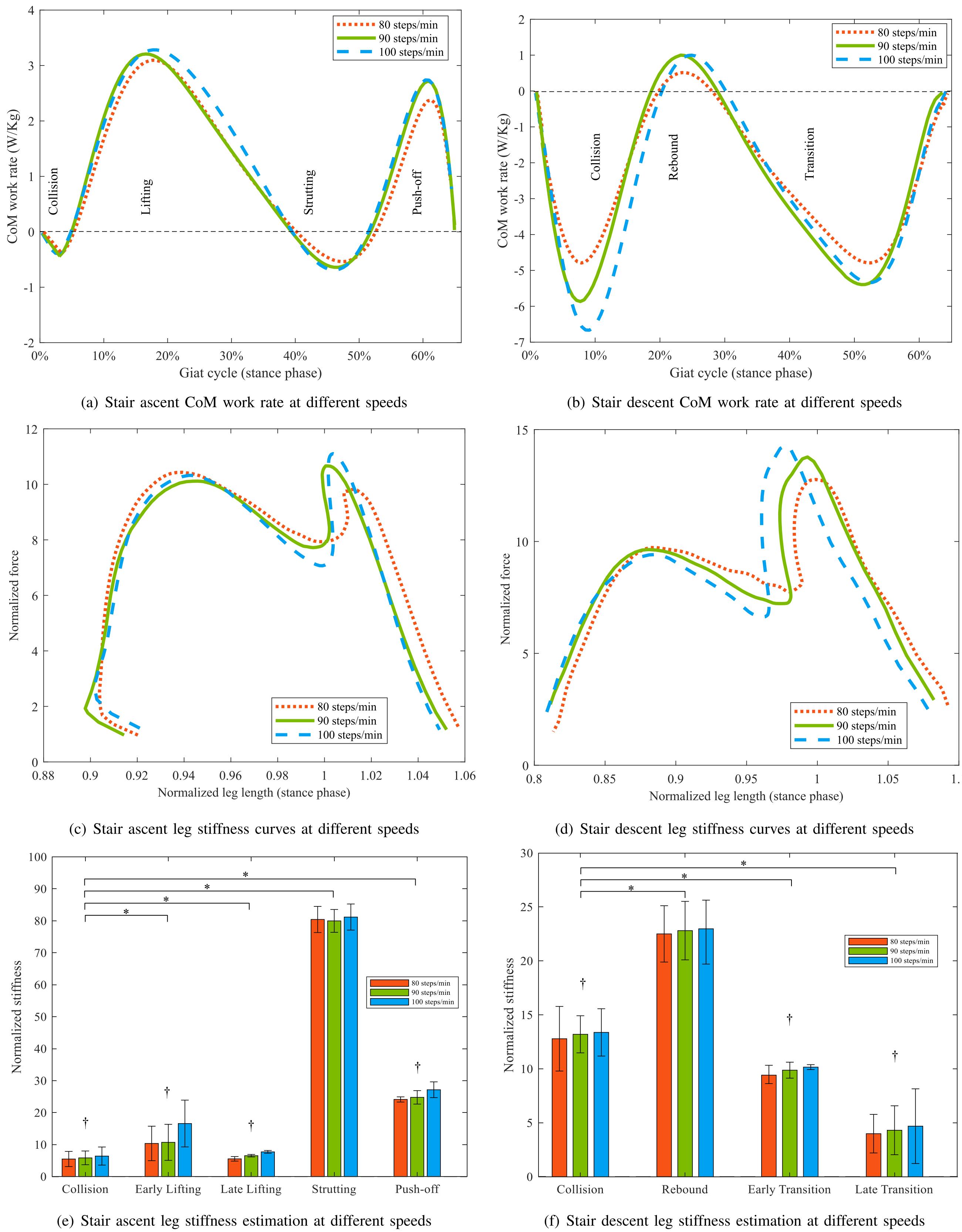

(a) Stair ascent CoM work rate at different speeds

(b) Stair descent CoM work rate at different speeds

(c) Stair ascent leg stiffness curves at different speeds

(d) Stair descent leg stiffness curves at different speeds

(e) Stair ascent leg stiffness estimation at different speeds

(f) Stair descent leg stiffness estimation at different speeds

Fig. 5. Stair ascent and descent at different speeds. (a) and (c) are CoM work rate and $F_N - L_N$ curve at different speeds during stair ascent, respectively. (b) and (d) are CoM work rate and $F_N - L_N$ curve at different speeds during stair descent, respectively. (e) and (f) are leg stiffness at different gait speeds in different gait phases during stair ascent and descent, respectively. Symbol † indicates speed effect and * indicates phase effect for both groups at $p < 0.05$.

IV. Discussion

A. Unification of Leg Stiffness and CoM in Phase Subdivision of Stair Climbing

According to the dividing method of the stance phase, each trial of every subject can be divided into several subphases for analysis. The benefit of dividing the stance phase into subphases is that it is obvious and comparable to discover the differences among numerous walking gaits from the view of the support leg, shown in the subphases curve characteristics, including the slopes and values. Moreover, the work behavior of the support leg is related to the performance of the CoM work, which can be shown in the CoM work rate curve.

Two widely used methods exist to define the gait cycle during level walking, that is, CoM work rate and gait events. In this study, we aimed to discover the change of mechanical energy and leg stiffness during stair ascent and descent, and define the stair climbing gait cycle based on this kinetic and kinematic information. First, we compared the cutoff moments of the subphases. During the stance phase of stair ascent, by the CoM work rate method, the four subphases' cutoff moments were approximately 4%, 37%, and 48%. When synchronizing the CoM work rate and $F_N - L_N$ curve, the cutoff moments in the $F_N - L_N$ curve were 6%, 36%, and 50%, respectively. The two methods' cutoff moments are similar throughout the entire support gait cycle. If the gait phases are not used strictly, the two methods' moments can be cut off in an averaged manner, for example, roughly 5%, 40%, and 50% corresponding, respectively, to the aforementioned cutoff moments. Through the correspondence between the CoM and the leg stiffness curve, it is proved that the gait cycle divided according to the change of stiffness is feasible and significant. The CoM work rate method divides the stance phase referring to human energy, which can indicate the mechanical energy change and the work transition directly. The gait events method follows the actual lower-limb motions, truly and clearly reflecting the gait kinematics. Thus, the two methods meet different specific demands of gait analysis. The stair climbing gait cycle subdivision method proposed in this paper is simple and integrated, and can reflect the relationship between the leg stiffness and the CoM work rate. The benefit of this description is that it combines many biomechanical characteristics in a single curve. By observing and analyzing the $F_N - L_N$ curve, the walking support leg stiffness can be described as the form of the force-displacement curve or equation, which changes the value and direction during the entire stance phase.

B. Implications for Prostheses or Exoskeleton Control

When designing a stair climbing controller for a prosthesis or exoskeleton, similar to level walking, it is also necessary to divide the gait phases of stair ascent and descent. In this study, the gait cycles for stair climbing were divided according to the leg stiffness characteristics corresponding to the different segments of the curve. A segmental linear fitting to the curve was performed to obtain the corresponding equations. For example, the curve of the collision phase can be represented by the following equation:

$$F_N = 6.561 L_N + 6.152. \tag{5}$$

Furthermore, to mimic the leg stiffness of healthy people, a spring-loaded inverted pendulum model can be used to design biomimetic control strategies for a wearable lower-extremity robot [40], which can be expressed by an impedance controller as follows:

$$F_l = k\,(L_l - L_r) + b\dot{L}_l, \tag{6}$$

where L_l represents the real-time length during stair climbing, L_r the desired length that can be referred to the data in this study, and $\dot{L}_l$ the rate of change in virtual limb length. k is the leg stiffness, which can be calculated by (4). b is the damping parameter, which can be tuned according to the walking performance of the rehabilitation devices. Based on the stiffness fitting equation of each phase, one can design a virtual impedance controller to realize different stiffness.

C. Limitations and Future Work

The methods used in this study rely on accurate estimation of virtual limb length. A limitation of this experiment is that it is difficult to determine the real position of the CoM during stair climbing. In this study, the position of the center of the pelvis was used to represent the position of the real CoM [46], which introduced a slight measuring error of the CoM position. Furthermore, the real position of the CoP at the beginning and end of the support phase may be affected by the disturbance of the force plate. When contacting the force plate, the z coordinates of both the CoP and the force plate are supposed to be the same. However, due to the heel strike and push-off action, the z coordinate of the CoP experiences obvious fluctuations during these two phases, which affects the estimation of length.

As shown in Fig. 5(c) and (d), it seems to be a difference in the F_N-L_N curve depending on cadence, and online identification of subphases also depends on gait speed. There seems to be a non-linear mapping between the leg stiffness and stair climbing speed. In our future work, non-linear function fitting or neural network methods may be used to approximate this non-linear mapping. Due to space limitations, we will continue to improve our theory and apply it to wearable lower-extremity robots.

References

[1] A. Young and D. Ferris, "State of the art and future directions for lower limb robotic exoskeletons," *IEEE Trans. Neural Syst. Rehabil. Eng.*, vol. 25, no. 2, pp. 171–182, Mar. 2016.

[2] Z. Li *et al.*, "Hybrid brain/muscle signals powered wearable walking exoskeleton enhancing motor ability in climbing stairs activity," *IEEE Trans. Med. Robot. Bionics*, vol. 1, no. 4, pp. 218–227, Nov. 2019.

[3] Y. Li, Y. Wu, Y. Zeng, and D. Gu, "Biomechanical differences before and after arthroscopic partial meniscectomy in patients with semilunar and discoid lateral meniscus injury," *Amer. J. Transl. Res.*, vol. 12, no. 6, p. 2793, 2020.

[4] Z. Li, C. Deng, and K. Zhao, "Human-cooperative control of a wearable walking exoskeleton for enhancing climbing stair activities," *IEEE Trans. Ind. Electron.*, vol. 67, no. 4, pp. 3086–3095, Apr. 2020.

[5] J. T. Lee and M. Goldfarb, "Effect of a swing-assist knee prosthesis on stair ambulation," *IEEE Trans. Neural Syst. Rehabil. Eng.*, vol. 29, pp. 2046–2054, 2021.

[6] T. Lenzi, M. Cempini, L. J. Hargrove, and T. A. Kuiken, "Design, development, and validation of a lightweight nonbackdrivable robotic ankle prosthesis," *IEEE/ASME Trans. Mechatronics*, vol. 24, no. 2, pp. 471–482, Apr. 2019.

[7] S. Culver, H. Bartlett, A. Shultz, and M. Goldfarb, "A stair ascent and descent controller for a powered ankle prosthesis," *IEEE Trans. Neural Syst. Rehabil. Eng.*, vol. 26, no. 5, pp. 993–1002, Mar. 2018.

[8] K. Zhang *et al.*, "Environmental features recognition for lower limb prostheses toward predictive walking," *IEEE Trans. Neural Syst. Rehabil. Eng.*, vol. 27, no. 3, pp. 465–476, Mar. 2019.

[9] K. Zhang *et al.*, "A subvision system for enhancing the environmental adaptability of the powered transfemoral prosthesis," *IEEE Trans. Cybern.*, vol. 51, no. 6, pp. 3285–3297, Jun. 2021.

[10] J. Liu, C. Xiong, and C. Fu, "An ankle exoskeleton using a lightweight motor to create high power assistance for push-off," *J. Mech. Robot.*, vol. 11, no. 4, Aug. 2019, Art. no. 041001.

[11] A. J. Young, A. M. Simon, and L. J. Hargrove, "A training method for locomotion mode prediction using powered lower limb prostheses," *IEEE Trans. Neural Syst. Rehabil. Eng.*, vol. 22, no. 3, pp. 671–677, May 2014.

[12] T. R. Clites, M. K. Shepherd, K. A. Ingraham, L. Wontorcik, and E. J. Rouse, "Understanding patient preference in prosthetic ankle stiffness," *J. Neuroeng. Rehabil.*, vol. 18, no. 1, pp. 1–16, Dec. 2021.

[13] L. Ma, Y. Leng, W. Jiang, Y. Qian, and C. Fu, "Design an underactuated soft exoskeleton to sequentially provide knee extension and ankle plantarflexion assistance," *IEEE Robot. Autom. Lett.*, vol. 7, no. 1, pp. 271–278, Jan. 2022.

[14] A. Ekelem, G. Bastas, C. M. Durrough, and M. Goldfarb, "Variable geometry stair ascent and descent controller for a powered lower limb exoskeleton," *J. Med. Devices*, vol. 12, no. 3, Sep. 2018, Art. no. 031009.

[15] Y. Chang, W. Wang, and C. Fu, "A lower limb exoskeleton recycling energy from knee and ankle joints to assist push-off," *J. Mech. Robot.*, vol. 12, no. 5, Oct. 2020, Art. no. 051011.

[16] J. Camargo, A. Ramanathan, W. Flanagan, and A. Young, "A comprehensive, open-source dataset of lower limb biomechanics in multiple conditions of stairs, ramps, and level-ground ambulation and transitions," *J. Biomech.*, vol. 119, Apr. 2021, Art. no. 110320.

[17] S. Vallabhajosula, J. M. Yentes, M. Momcilovic, D. J. Blanke, and N. Stergiou, "Do lower-extremity joint dynamics change when stair negotiation is initiated with a self-selected comfortable gait speed?" *Gait Posture*, vol. 35, no. 2, pp. 203–208, Feb. 2012.

[18] J. K. Startzell, D. A. Owens, L. M. Mulfinger, and P. R. Cavanagh, "Stair negotiation in older people: A review," *J. Amer. Geriatrics Soc.*, vol. 48, no. 5, pp. 567–580, May 2000.

[19] J. Peng, N. P. Fey, T. A. Kuiken, and L. J. Hargrove, "Anticipatory kinematics and muscle activity preceding transitions from level-ground walking to stair ascent and descent," *J. Biomech.*, vol. 49, no. 4, pp. 528–536, 2016.

[20] E. H. Sinitski, A. H. Hansen, and J. M. Wilken, "Biomechanics of the ankle–foot system during stair ambulation: Implications for design of advanced ankle–foot prostheses," *J. Biomech.*, vol. 45, no. 3, pp. 588–594, Feb. 2012.

[21] A. Bergland, H. Sylliaas, G. B. Jarnlo, and T. B. Wyller, "Health, balance, and walking as correlates of climbing steps," *J. Aging Phys. Activity*, vol. 16, no. 1, pp. 42–52, Jan. 2008.

[22] R. C. Sheehan and J. S. Gottschall, "At similar angles, slope walking has a greater fall risk than stair walking," *Appl. Ergonom.*, vol. 43, no. 3, pp. 473–478, May 2012.

[23] P. A. Costigan, K. J. Deluzio, and U. P. Wyss, "Knee and hip kinetics during normal stair climbing," *Gait Posture*, vol. 16, no. 1, pp. 31–37, Aug. 2002.

[24] J. M. Wilken, E. H. Sinitski, and E. A. Bagg, "The role of lower extremity joint powers in successful stair ambulation," *Gait Posture*, vol. 34, no. 1, pp. 142–144, May 2011.

[25] R. A. Wervey, G. F. Harris, and J. J. Wertsch, "Plantar pressure characteristics during stair climbing and descent," in *Proc. 19th Ann. Int. Conf. IEEE EBMS*, vol. 4, Oct. 1997, pp. 1746–1748.

[26] K. A. Hamel, N. Okita, J. S. Higginson, and P. R. Cavanagh, "Foot clearance during stair descent: Effects of age and illumination," *Gait Posture*, vol. 21, no. 2, pp. 135–140, Feb. 2005.

[27] A. K. Silverman, R. R. Neptune, E. H. Sinitski, and J. M. Wilken, "Whole-body angular momentum during stair ascent and descent," *Gait Posture*, vol. 39, no. 4, pp. 1109–1114, Apr. 2014.

[28] A. Stacoff, C. Diezi, G. Luder, E. Stüssi, and I. A. Kramers-de-Quervain, "Ground reaction forces on stairs: Effects of stair inclination and age," *Gait Posture*, vol. 21, no. 1, pp. 24–38, Jan. 2005.

[29] S. Vallabhajosula, C. W. Tan, M. Mukherjee, A. J. Davidson, and N. Stergiou, "Biomechanical analyses of stair-climbing while dual-tasking," *J. Biomech.*, vol. 48, no. 6, pp. 921–929, Apr. 2015.

[30] R. Riener, M. Rabuffetti, and C. Frigo, "Stair ascent and descent at different inclinations," *Gait Posture*, vol. 15, no. 1, pp. 32–44, 2002.

[31] S. Vallabhajosula, J. M. Yentes, and N. Stergiou, "Frontal joint dynamics when initiating stair ascent from a walk versus a stand," *J. Biomech.*, vol. 45, no. 3, pp. 609–613, Feb. 2012.

[32] H. A. Ojha, R. W. Kern, C.-H.-J. Lin, and C. J. Winstein, "Age affects the attentional demands of stair ambulation: Evidence from a dual-task approach," *Phys. Therapy*, vol. 89, no. 10, pp. 1080–1088, Oct. 2009.

[33] T. Schmalz, S. Blumentritt, and B. Marx, "Biomechanical analysis of stair ambulation in lower limb amputees," *Gait Posture*, vol. 25, no. 2, pp. 267–278, Feb. 2007.

[34] J. L. Asay, A. Mündermann, and T. P. Andriacchi, "Adaptive patterns of movement during stair climbing in patients with knee osteoarthritis," *J. Orthopaedic Res.*, vol. 27, no. 3, pp. 325–329, Mar. 2009.

[35] J. E. Zachazewski, P. O. Riley, and D. E. Krebs, "Biomechanical analysis of body mass transfer during stair ascent and descent of healthy subjects," *J. Rehabil. Res. Dev.*, vol. 30, p. 412, Jan. 1993.

[36] C. T. Farley and O. González, "Leg stiffness and stride frequency in human running," *J. Biomech.*, vol. 29, no. 2, pp. 181–186, Feb. 1996.

[37] R. J. Butler, H. P. Crowell, III, and I. M. Davis, "Lower extremity stiffness: Implications for performance and injury," *Clin. Biomech.*, vol. 18, no. 6, pp. 511–517, Jul. 2003.

[38] A.-R. Akl, A. Baca, J. Richards, and F. Conceição, "Leg and lower limb dynamic joint stiffness during different walking speeds in healthy adults," *Gait Posture*, vol. 82, pp. 294–300, Oct. 2020.

[39] H. Hong, S. Kim, C. Kim, S. Lee, and S. Park, "Spring-like gait mechanics observed during walking in both young and older adults," *J. Biomech.*, vol. 46, no. 1, pp. 77–82, Jan. 2013.

[40] D. R. Coleman, D. Cannavan, S. Horne, and A. J. Blazevich, "Leg stiffness in human running: Comparison of estimates derived from previously published models to direct kinematic–kinetic measures," *J. Biomech.*, vol. 45, no. 11, pp. 1987–1991, Jul. 2012.

[41] Y. Blum, S. W. Lipfert, and A. Seyfarth, "Effective leg stiffness in running," *J. Biomech.*, vol. 42, no. 14, pp. 2400–2405, Oct. 2009.

[42] H. Hobara, K. Inoue, T. Muraoka, K. Omuro, M. Sakamoto, and K. Kanosue, "Leg stiffness adjustment for a range of hopping frequencies in humans," *J. Biomech.*, vol. 43, no. 3, pp. 506–511, Feb. 2010.

[43] L. C. Visser, S. Stramigioli, and R. Carloni, "Control strategy for energy-efficient bipedal walking with variable leg stiffness," in *Proc. IEEE Int. Conf. Robot. Automat.*, May 2013, pp. 5644–5649.

[44] A. Silder, T. Besier, and S. L. Delp, "Running with a load increases leg stiffness," *J. Biomech.*, vol. 48, no. 6, pp. 1003–1008, Apr. 2015.

[45] B. J. McFadyen and D. A. Winter, "An integrated biomechanical analysis of normal stair ascent and descent," *J. Biomech.*, vol. 21, no. 9, pp. 733–744, Jan. 1988.

[46] L. Forsyth, S. Roeles, and C. Childs, "Efficacy of using the pelvic method to estimate centre of mass position in response to gait perturbations," in *Proc. 8th World Congr. Biomech.*, 2018, p. 1.

[47] K. E. Zelik and A. D. Kuo, "Human walking isn't all hard work: Evidence of soft tissue contributions to energy dissipation and return," *J. Exp. Biol.*, vol. 213, no. 24, pp. 4257–4264, Dec. 2010.

[48] Y. Leng, X. Lin, Z. Lu, A. Song, Z. Yu, and C. Fu, "A model to predict ground reaction force for elastically-suspended backpacks," *Gait Posture*, vol. 82, pp. 118–125, Oct. 2020.

[49] J. M. Donelan, R. Kram, and A. D. Kuo, "Simultaneous positive and negative external mechanical work in human walking," *J. Biomech.*, vol. 35, no. 1, pp. 117–124, Jan. 2002.

[50] Y. Leng, X. Lin, L. Yang, K. Zhang, X. Chen, and C. Fu, "A model for estimating the leg mechanical work required to walk with an elastically suspended backpack," *IEEE Trans. Human-Machine Syst.*, early access, Jan. 11, 2022, doi: 10.1109/THMS.2021.3137012.

[51] M. L. Latash and V. M. Zatsiorsky, "Joint stiffness: Myth or reality?" *Hum. Movement Sci.*, vol. 12, no. 6, pp. 653–692, 1993.

[52] E. J. Rouse, R. D. Gregg, L. J. Hargrove, and J. W. Sensinger, "The difference between stiffness and quasi-stiffness in the context of biomechanical modeling," *IEEE Trans. Biomed. Eng.*, vol. 60, no. 2, pp. 562–568, Feb. 2013.

[53] S. Kim and S. Park, "Leg stiffness increases with speed to modulate gait frequency and propulsion energy," *J. Biomech.*, vol. 44, no. 7, pp. 1253–1258, Apr. 2011.